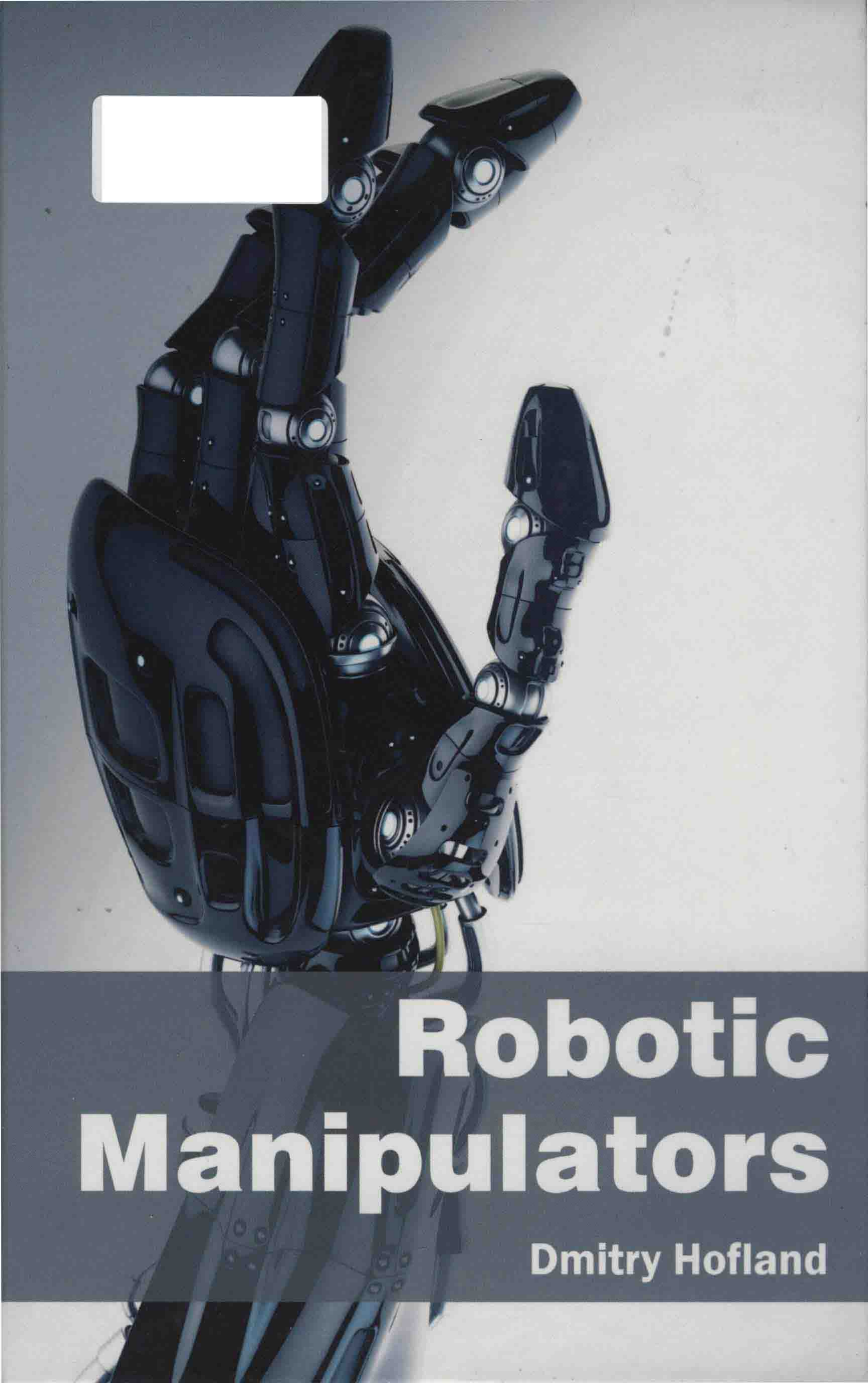

Robotic Manipulators

Dmitry Hofland

Robotic Manipulators

Edited by **Dmitry Hofland**

NY RESEARCH PRESS

New York

Published by NY Research Press,
23 West, 55th Street, Suite 816,
New York, NY 10019, USA
www.nyresearchpress.com

Robotic Manipulators
Edited by Dmitry Hofland

International Standard Book Number: 978-1-63238-402-7 (Hardback)

Printed in China.

Robotic Manipulators

Preface

This book aims to highlight the current researches and provides a platform to further the scope of innovations in this area. This book is a product of the combined efforts of many researchers and scientists, after going through thorough studies and analysis from different parts of the world. The objective of this book is to provide the readers with the latest information of the field.

This book includes contributions of prominent researchers and engineers dealing with robotics and its related aspects. In the past few decades, interest in robotics has notably increased which has led to the advancement of theoretical research and products in this field. Robotics form an essential part of modern engineering and is associated with various other fields namely mathematics, mechanism design, computer and electric & electronics. The book extensively covers optimization modeling.

I would like to express my sincere thanks to the authors for their dedicated efforts in the completion of this book. I acknowledge the efforts of the publisher for providing constant support. Lastly, I would like to thank my family for their support in all academic endeavors.

Editor

Contents

Optimization

1

Nonlinear Dynamic Control and Friction Compensation of Parallel Manipulators

Weiwei Shang and Shuang Cong
University of Science and Technology of China
P.R. China

1. Introduction

Comparing with the serial ones, parallel manipulators have potential advantages in terms of high stiffness, accuracy and speed (Merlet, 2001). Especially the high accuracy and speed performances make the parallel manipulators widely applied to the following fields, like the pick-and-place operation in food, medicine, electronic industry and so on. At present, the key issues are the ways to meet the demand of high accuracy in moving process under the condition of high speed. In order to realize the high speed and accuracy motion, it's very important to design efficient control strategies for parallel manipulators.

In literatures, there are two basic control strategies for parallel manipulators (Zhang et.al., 2007): kinematic control strategies and dynamic control strategies. In the kinematic control strategies, parallel manipulators are decoupled into a group of single axis control systems, so they can be controlled by a group of individual controllers. Proportional-derivative (PD) control(Ghorbel et.al., 2000; Wu et.al., 2002), nonlinear PD (NPD) control (Ouyang et.al., 2002; Su et.al., 2004), and fuzzy control (Su et.al., 2005) all belong to this type of control strategies. These controllers do not always produce high control performance, and there is no guarantee of stability at the high speed. Unlike the kinematic control strategies, full dynamic model of parallel manipulators is taken into account in the dynamic control strategies. So the nonlinear dynamics of parallel manipulators can be compensated and better performance can be achieved with the dynamic strategies.

The traditional dynamic control strategies of parallel manipulators are the augmented PD (APD) control and the computed-torque (CT) control (Li & Wu, 2004; Cheng et.al., 2003; Paccot et.al., 2009). In the APD controller (Cheng et.al., 2003), the control law contains the tracking control term and the feed-forward compensation term. The tracking control term is realized by the PD control algorithm. The feed-forward compensation term contains the dynamic compensation calculated by the desired velocity and desired acceleration on the basis of the dynamic model. Compared with the simple PD controller, the APD controller is a tracking control method. However, the feed-forward compensation can not restrain the trajectory disturbance effectively, thus the tracking accuracy of the APD controller will be decreased. In order to solve this problem, the CT controller including the velocity feed-back is proposed based on the PD controller (Paccot et.al., 2009). The CT control method yields a controller that suppresses disturbance and tracks desired trajectories uniformly in all configurations of the manipulators. Both the APD controller and the CT controller contain two parts including the PD control term and the dynamic compensation term. For the presence of nonlinear factors such as modeling error and nonlinear friction in the dynamic models of the parallel manipulators, those traditional controllers can not achieve good control accuracy.

In order to overcome the uncertain factors in parallel manipulators, nonlinear control methods and friction compensation method are developed in this chapter. Firstly, in order to restrain the modeling error of parallel manipulators, a nonlinear PD (NPD) control algorithm is used to the APD controller, and a so-called augmented NPD (ANPD) controller is designed. Secondly, considering the feed-forward compensation term in the ANPD controller can not restrict the external disturbance, and the tracking accuracy will be affected when the disturbance exists. Thus the NPD controller is combined with the CT controller further, and a new control method named nonlinear CT (NCT) controller is developed. Thirdly, in order to compensate the nonlinear friction of parallel manipulators, a nonlinear model with two-sigmoid-function is introduced to modeling the nonlinear friction. This nonlinear friction model enables reconstruction of viscous, Coulomb, and Stribeck friction effects of parallel manipulators, and the nonlinear optimization tool is used to estimate the parameters in this model. In addition to the theoretical development, all the proposed methods in this chapter are validated on an actual parallel manipulator. The experiment results indicate that, compared with the conventional controllers, the proposed ANPD and NCT controller can get better trajectory tracking accuracy of the end-effector. Moreover, the experiment results also demonstrate that the nonlinear friction model is more accurately to compensate the friction, and is robust against the trajectory and the velocity changes.

2. Dynamic modelling

The experiment platform is a 2-DOF parallel manipulator with redundant actuation. As shown in Fig. 1, a reference frame is established in the workspace of the parallel manipulator. The unit of the frame is meter. The parallel manipulator is actuated by three servo motors located at the base A1, A2, and A3, and the end-effector is mounted at the common joint O, where the three chains meet. Coordinates of the three bases are A1 (0, 0.25), A2 (0.433, 0), and A3 (0.433, 0.5), and all of the links have the same length $l = 0.244$ m. The definitions of the joint angles are shown in the Fig. 1, q_{a1}, q_{a2}, q_{a3} refer to the active joint angles and q_{b1}, q_{b2}, q_{b3} refer to the passive joint angles.

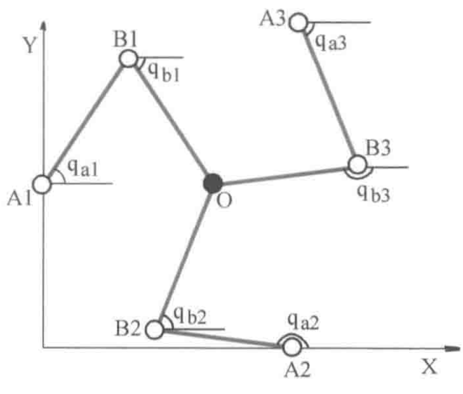

Fig. 1. Coordinates of the 2-DOF parallel manipulator with redundant actuation

Cutting the parallel manipulator at the common point O in Fig. 1, one can have an open-chain system including three independent planar 2-DOF serial manipulators, each of which contains an active joint and a passive joint. The dynamic model of the parallel manipulator equals to the model of the open-chain system plus the closed-loop constraints, thus the dynamic model of the whole parallel manipulator can be formulated by combining the dynamics of the three serial manipulators under the constraints.
As we know, the dynamic model of each planar 2-DOF serial manipulator can be formulated as (Murray et.al., 1994)

$$\mathbf{M}_i\ddot{\mathbf{q}}_i + \mathbf{C}_i\dot{\mathbf{q}}_i + \mathbf{f}_i = \boldsymbol{\tau}_i \tag{1}$$

where $\mathbf{q}_i = [q_{ai} \quad q_{bi}]^T$, q_{ai} and q_{bi} are the active joint and passive joint angle, respectively; $\mathbf{M}_i$ is inertia matrix, and $\mathbf{C}_i$ is Coriolis and centrifugal force matrix, which are defined as

$$\mathbf{M}_i = \begin{bmatrix} \alpha_i & \gamma_i \cos(q_{ai} - q_{bi}) \\ \gamma_i \cos(q_{ai} - q_{bi}) & \beta_i \end{bmatrix}$$

$$\mathbf{C}_i = \begin{bmatrix} 0 & \gamma_i \sin(q_{ai} - q_{bi})\dot{q}_{bi} \\ -\gamma_i \sin(q_{ai} - q_{bi})\dot{q}_{ai} & 0 \end{bmatrix}$$

where $\alpha_i, \beta_i, \gamma_i$, $i = 1,2,3$ are the dynamic parameters which are related with the physical parameters such as mass, center of mass, and inertia. In Eq.(1), $\boldsymbol{\tau}_i = [\tau_{ai} \quad \tau_{bi}]^T$ is joint torque vector, where τ_{ai} is the active joint torque, the passive joint torque $\tau_{bi} = 0$. Vector $\mathbf{f}_i = [f_{ai} \quad f_{bi}]^T$ is the friction torque, where f_{ai} and f_{bi} are the active joint friction and passive joint friction, respectively. The friction parameters of the active joints and the passive joints are identified simultaneously for the parallel manipulator (Shang et.al., 2010). And from the identified results, one can find that the friction parameters of the passive joints are much smaller than those of the active joints. Thus, compared with the active joints friction f_{ai}, the passive joint friction f_{bi} is much smaller and it can be neglected (Shang et.al., 2010). Generally, the active joint friction torque f_{ai} can be formulated by using the Coulomb + viscous friction model as

$$f_{ai} = sign(\dot{q}_{ai}) f_{ci} + f_{vi}\dot{q}_{ai} \tag{2}$$

where f_{ci} represents the Coulomb friction, and f_{vi} represents the coefficient of the viscous friction.
Combining the dynamic models of three 2-DOF serial manipulators, the dynamic model of the open-chain system can be expressed as

$$\mathbf{M}\ddot{\mathbf{q}} + \mathbf{C}\dot{\mathbf{q}} + \mathbf{f} = \boldsymbol{\tau} \tag{3}$$

where the definition of the symbols is similar to those in Eq.(1), only the difference is that the symbols in Eq.(3) represent the whole open-chain system not a 2-DOF serial manipulator. Based on Eq.(3) of the open-chain system and the constraint forces due to the closed-loop constraints, the dynamic model of the parallel manipulator can be written as

$$\mathbf{M}\ddot{\mathbf{q}} + \mathbf{C}\dot{\mathbf{q}} + \mathbf{f} = \boldsymbol{\tau} + \mathbf{A}^T\boldsymbol{\lambda} \tag{4}$$

where $\mathbf{A}^T\boldsymbol{\lambda}$ represents the constraint force vector, here matrix $\mathbf{A}$ is the differential of the closed-loop constrained equation and $\boldsymbol{\lambda}$ is a unknown multiplier representing the magnitude of the constraint forces. Fortunately, $\mathbf{A}^T\boldsymbol{\lambda}$ can be eliminated, by finding the null-space of matrix $\mathbf{A}$ (Muller, 2005). With the Jacobian matrix $\mathbf{W}$, we have

$$\dot{\mathbf{q}} = \mathbf{W}\dot{\mathbf{q}}_e \tag{5}$$

where $\dot{\mathbf{q}} = [\dot{q}_{a1} \quad \dot{q}_{a2} \quad \dot{q}_{a3} \quad \dot{q}_{b1} \quad \dot{q}_{b2} \quad \dot{q}_{b3}]^T$ represents the velocity vector of all the joints, $\dot{\mathbf{q}}_e = [\dot{q}_x \quad \dot{q}_y]^T$ represents the velocity vector of the end-effector, and the Jacobian matrix $\mathbf{W}$ is defined as

$$\mathbf{W} = \begin{bmatrix} r_1\cos(q_{b1}) & r_1\sin(q_{b1}) \\ r_2\cos(q_{b2}) & r_2\sin(q_{b2}) \\ r_3\cos(q_{b3}) & r_3\sin(q_{b3}) \\ -r_1\cos(q_{a1}) & -r_1\sin(q_{a1}) \\ -r_2\cos(q_{a2}) & -r_2\sin(q_{a2}) \\ -r_3\cos(q_{a3}) & -r_3\sin(q_{a3}) \end{bmatrix}, \text{ where } r_i = \frac{1}{l\sin(q_{bi} - q_{ai})}$$

Considering the constraint equation $\mathbf{A}\dot{\mathbf{q}} = \mathbf{0}$, then one can have $\mathbf{AW}\dot{\mathbf{q}}_\mathbf{e} = \mathbf{0}$ with the Jacobian relation Eq.(5). The velocity vector $\dot{\mathbf{q}}_e$ of the end-effector contains independent generalized coordinates, so one can get $\mathbf{AW} = \mathbf{0}$, or equivalently, $\mathbf{W}^T\mathbf{A}^T = \mathbf{0}$. With this result, the term of $\mathbf{A}^T\boldsymbol{\lambda}$ can be eliminated, and the dynamic model Eq. (4) can be written as

$$\mathbf{W}^T\mathbf{M}\ddot{\mathbf{q}} + \mathbf{W}^T\mathbf{C}\dot{\mathbf{q}} + \mathbf{W}^T\mathbf{f} = \mathbf{W}^T\boldsymbol{\tau} + \mathbf{W}^T\mathbf{A}^T\boldsymbol{\lambda} = \mathbf{W}^T\boldsymbol{\tau} \tag{6}$$

In order to study dynamic control and trajectory planning of the parallel manipulator both in the task space, we will further formulate the dynamic model in the task space on the basis of the dynamic model Eq. (6) of the joint space. Differentiating the Jacobian Eq. (5) yields

$$\ddot{\mathbf{q}} = \dot{\mathbf{W}}\dot{\mathbf{q}}_e + \mathbf{W}\ddot{\mathbf{q}}_e \tag{7}$$

and substituting Eqs. (5) and (7) into Eq. (6), the dynamic model in the task space can be written as

$$\mathbf{W}^T\mathbf{MW}\ddot{\mathbf{q}}_e + \mathbf{W}^T(\mathbf{M}\dot{\mathbf{W}} + \mathbf{CW})\dot{\mathbf{q}}_e + \mathbf{W}^T\mathbf{f} = \mathbf{W}^T\boldsymbol{\tau} \tag{8}$$

If the friction torques of the passive joints is neglected, then Eq. (8) can be further simplified. Let $\boldsymbol{\tau}_a$ and $\mathbf{f}_a$ be the actuator and friction torque vector of the three active joints respectively, then $\mathbf{W}^T\boldsymbol{\tau} = \mathbf{S}^T\boldsymbol{\tau}_a$, and $\mathbf{W}^T\mathbf{f} = \mathbf{S}^T\mathbf{f}_a$. Here, $\mathbf{S}$ is the Jacobian matrix between the velocity of the end-effector and the velocity of three active joints, and $\mathbf{S}$ is written as

$$\mathbf{S} = \begin{bmatrix} r_1\cos(q_{b1}) & r_1\sin(q_{b1}) \\ r_2\cos(q_{b2}) & r_2\sin(q_{b2}) \\ r_3\cos(q_{b3}) & r_3\sin(q_{b3}) \end{bmatrix}$$

Then, the dynamic model in the task space can be written as

$$\mathbf{W}^T\mathbf{M}\mathbf{W}\ddot{\mathbf{q}}_e + \mathbf{W}^T(\mathbf{M}\dot{\mathbf{W}} + \mathbf{C}\mathbf{W})\dot{\mathbf{q}}_e + \mathbf{S}^T\mathbf{f}_a = \mathbf{S}^T\boldsymbol{\tau}_a \tag{9}$$

The above Eq.(9) can be briefly expressed as

$$\mathbf{M}_e\ddot{\mathbf{q}}_e + \mathbf{C}_e\dot{\mathbf{q}}_e + \mathbf{S}^T\mathbf{f}_a = \mathbf{S}^T\boldsymbol{\tau}_a \tag{10}$$

where $\mathbf{M}_e = \mathbf{W}^T\mathbf{M}\mathbf{W}$ is the inertial matrix in the task space, and $\mathbf{C}_e = \mathbf{W}^T(\mathbf{M}\dot{\mathbf{W}} + \mathbf{C}\mathbf{W})$ is the Coriolis and centrifugal force matrix in the task space.

The dynamic model Eq. (10) in the task space also satisfies the similar structural properties to the dynamic model of the open-chain system and the 2-DOF serial manipulator as follows (Cheng et.al., 2003):

a. $\mathbf{M}_e$ is symmetric and positive.

b. $\dot{\mathbf{M}}_e - 2\mathbf{C}_e$ is skew-symmetric matrix.

3. Nonlinear dynamic control by using the NPD

There are two conventional dynamic controllers for parallel manipulators: APD controller and CT controller. The common feature of the two controllers is eliminating the tracking error by linear PD control. However, the linear PD control is not robust against the uncertain factors such as modeling error and external disturbance. To overcome this problem, the NPD control can be combined with the conventional control strategies to improve the control accuracy and disturbance rejection ability.

3.1 NPD controller

As well as we know, the linear PD controller takes the form

$$u_L(t) = k_p e(t) + k_d \dot{e}(t) \tag{11}$$

where k_p and k_d are the proportional and derivative constants respectively, and $e(t)$ is the system error.

The nonlinear PD (NPD) controller has a similar structure as the linear PD controller (11), the NPD controller may be any control structure of the form

$$u_N(t) = k_p(\cdot)e(t) + k_d(\cdot)\dot{e}(t) \tag{12}$$

where $k_p(\cdot)$ and $k_d(\cdot)$ are the time-varying proportional and derivative gains, which may depend on system state, input or other variables.

Currently, several NPD controllers have been proposed for robotic application (Xu et.al., 1995; Kelly & Ricardo, 1996; Seraji et.al., 1998). The NPD controller has superior trajectory tracking and disturbance rejection ability compared with the linear PD controllers for robot control. The NPD controller proposed by Han has a simple structure as (Han, 1994)

$$u_H(t) = k_p fun(e(t), \alpha_1, \delta_1) + k_d fun(\dot{e}(t), \alpha_2, \delta_2) \tag{13}$$

where the function fun can be defined as

$$fun(x,\alpha,\delta)=\begin{cases}|x|^{\alpha}sign(x), & |x|>\delta\\ x/\delta^{1-\alpha}, & |x|\le\delta\end{cases} \tag{14}$$

where α refers to the nonlinearity, specially the NPD will degenerate into the linear PD when $\alpha=1$; δ refers to the threshold of the error (or error derivative), and it is at the same magnitude with the error (or error derivative). The NPD controller (13) can be rewritten as the form (12), then $k_p(\cdot)$ can be derived as

$$k_p(e)=\begin{cases}k_p|e|^{\alpha_1-1} & |e|>\delta_1\\ k_p{\delta_1}^{\alpha_1-1} & |e|\le\delta_1\end{cases} \tag{15}$$

Similarly, $k_d(\cdot)$ can be expressed as

$$k_d(\dot{e})=\begin{cases}k_d|\dot{e}|^{\alpha_2-1} & |\dot{e}|>\delta_2\\ k_d{\delta_2}^{\alpha_2-1} & |\dot{e}|\le\delta_2\end{cases} \tag{16}$$

In (15) and (16), α_1 and α_2 can be determined in the interval [0.5, 1.0] and [1.0, 1.5], respectively. This choice makes the nonlinear gains with the following characteristics (Han, 1994): on one hand, large gain for small error and small gain for large error; on the other hand, large gain for large error rate and small gain for small error rate. Such variations of the gains result in a rapid transition of the systems with favorable damping. In addition, the NPD controller is robust against the changes of the system parameters and the nonlinear factors. Thus the NPD controller (13) is suitable to the trajectory tracking of the high-speed planar parallel manipulator.

3.2 Augmented NPD controller

The augmented NPD (ANPD) controller developed here is designed by replacing the linear PD in the APD controller with the NPD algorithm. According to the APD controller and the NPD control algorithm (13), based on the dynamic model (10), the control law of the ANPD controller can be written as (Shang et.al., 2009)

$$\tau_A=\mathbf{M}_e\ddot{\mathbf{q}}_e^d+\mathbf{C}_e\dot{\mathbf{q}}_e^d+\mathbf{S}^T\mathbf{f}_a+\mathbf{K}_p(\mathbf{e})\mathbf{e}+\mathbf{K}_d(\dot{\mathbf{e}})\dot{\mathbf{e}} \tag{17}$$

where $\dot{\mathbf{q}}_e^d$ and $\ddot{\mathbf{q}}_e^d$ are the desired velocity and acceleration of the end-effector. The control law (17) can be divided into three terms according to different functions. The first term is the dynamics compensation defined by the desired trajectory, which can be written as

$$\tau_{A1}=\mathbf{M}_e\ddot{\mathbf{q}}_e^d+\mathbf{C}_e\dot{\mathbf{q}}_e^d \tag{18.a}$$

The second term is the friction compensation, which can be written as

$$\tau_{A2}=\mathbf{S}^T\mathbf{f}_a \tag{18.b}$$

The third term is the tracking error elimination, which can be written as

$$\tau_{A3}=\mathbf{K}_p(\mathbf{e})\mathbf{e}+\mathbf{K}_d(\dot{\mathbf{e}})\dot{\mathbf{e}} \tag{18.c}$$